Li *et al. Chin. J. Mech. Eng.* (2021) 34:26
https://doi.org/10.1186/s10033-021-00545-8

Chinese Journal of Mechanical Engineering

ORIGINAL ARTICLE

Open Access

Fabrication of Carbon Nanotubes and Rare Earth Pr Reinforced AZ91 Composites by Powder Metallurgy

Ning Li[1,2], Hong Yan[1*], Qingjie Wu[2] and Zeyu Cao[1]

Abstract

It can be known from a large number of research results that improving the dispersibility of CNTs can effectively optimize the mechanical properties of the corresponding metal matrix composites. However, the crucial issue of increasing the bonding of CNTs and the matrix is still unsolved. In this paper, a novel method was developed to increase interfacial bonding strength by coating titanium oxide (TiO_2) on the surface of CNTs. The rare earth Pr and TiO2@CNTs-reinforced AZ91matrix composites were successfully fabricated by powder metallurgy. Hot press sintering and hot extrusion of the milled powder was performed. After hot extrusion, the influence of TiO_2@CNTs on the microstructure and mechanical properties of the composites were investigated. The results showed that the coating process can improve the distribution of CNTs in Mg alloy. The CNTs refined the grains of the matrix, and the CNTs were presented throughout the extrusion direction. When the TiO_2@CNTs content was 1.0 wt.%, the yield strength (YS), ultimate tensile strength (UTS), and elongation of the alloy attained maximum values. The values were improved by 23.5%, 82.1%, and 40.0%, respectively, when compared with the AZ91 alloy. Good interfacial bonding was achieved, which resulted in an effective tensile loading transfer at the interface. CNTs carried the tensile stress and were observed on the tensile fracture.

Keywords: Carbon nanotubes, Titanium oxide, AZ91, Coating, Rare earth

1 Introduction

With the requirements of modern society for energy saving, light-weight properties and green environmental protection, the use of magnesium alloys is becoming more prevalent [1, 2]. However, magnesium alloys have lower absolute strength, lower wear resistance and poor corrosion resistance compared to other structural metals, which limits its application breadth. The development of magnesium-based composites can significantly improve the elastic modulus, wear resistance and high temperature resistance. Therefore, research of magnesium-based composites is highly significant. Rare earth elements have been widely used to strengthen magnesium alloys. The hardness, wear resistance, and corrosion resistance of AZ91 are improved by forming highly stable Al_2RE and $Al_{11}RE_3$ compounds [3, 4]. Small amounts of yttrium added to alloy AZ91 causes significant refinement of the microstructure, and the tensile properties and corrosion resistance were improved greatly [5]. With the addition of 0.75 wt.% Ce into AZ91D alloy, a comparable grain refinement can be achieved and an acicular phase $Al_{11}Ce_3$ is formed near the grain boundary [6]. Yield strength also increased after RE was added. With too much RE additions can cause the coarsening of $Al_{11}RE_3$ and have little benefit to the mechanical properties [7]. On the basis of rare earth magnesium alloys, how to further improve the performance of composite materials and generate wider applications have become popular research topics. The addition of carbon nanomaterials to reinforce the metal matrix composites is an alternative.

*Correspondence: hyan@ncu.edu.cn
[1] School of Mechanical Electrical Engineering, Nanchang University, Nanchang 330031, China
Full list of author information is available at the end of the article

Since the discovery of carbon nanotubes (CNTs), due to their high modulus of elasticity and tensile strength, they have been widely used as reinforcements for composite materials [8–10]. Carbon nanotubes were first used in the modification and enhancement of plastic polymers, and have been gradually applied and modified with metal matrix in recent decades. The improvement of carbon nanotubes for Mg matrix alloys is faced with two difficulties: 1) Carbon nanomaterials and Mg metal have poor wetting, difficult dispersion, and uneven distribution [11]; 2) While ensuring the structural integrity of the CNTs, a strong interface bond with the matrix is achieved. The fabrication of composites with uniformly distributed CNTs is difficult [12].

Hiroyuki Fukuda et al. [13, 14] produced an AZ61/CNT magnesium composite via powder metallurgy, and the addition of CNT was 0.74 vol.%. As a result, the tensile strength of the composite was improved. It was believed that the in situ formed Al_2MgC_2 compounds can optimize the grain structure to a certain extent. The strength and ductility of the nanocomposite were improved simultaneously. It was believed that CNTs can prevent local crack propagation to some extent. Liu and Li et al.'s research showed the strength and ductility of the nanocomposite were improved simultaneously due to the dispersion of CNTs and that depends on the solidification rate [15, 16]. When the solidification rate was high, the CNTs remained inside the grain. Compared with the magnesium matrix alloy, the ultimate tensile strength (UTS) and yield strength (YS) of the composite were significantly improved. The addition of CNTs leads to a reduced matrix grain and increased hardness, YS, and UTS of the AZ91D base alloy [17]. The tensile failure strain of AZ81 was increased with the addition of CNT [18]. The reasons were attributed to the following factors: (a) uniform distribution of CNT and (b) CNT-induced regulated precipitation of the MgAl second phase. Harun and Goh et al. [19, 20] added 0.5, 1, 2, and 4 wt.% CNTs in AZ61 alloy by mechanical ball milling, cold pressing, and hot extrusion. The results of the mechanical and corrosion tests showed that small additions of CNTs evidently improved the hardness and corrosion resistance of the composite, while increasing the CNT weight fraction resulted in a significant decrease in hardness, compression strength, wear rate, and corrosion resistance. C.S. It can be seen from the above literature that a large number of scholars use various processes to optimize the dispersion of CNTs in the matrix, and have effects of optimizing the mechanical properties of composites. However, the crucial issue of improving the bond between CNTs and the matrix has not been solved.

It can be found from our previous research [21] that the rare earth element, Pr, can improve the mechanical properties of an AZ91 alloy. Therefore, AZ91 was chosen as the matrix to investigate the effects of carbon nanotubes and Pr on the mechanical of the composites. Powder metallurgy and hot extrusion were used to improve the dispersibility of CNTs in alloy materials. The interfacial bonding strength between the CNT and the matrix material was improved by surface coating processing of the CNTs.

2 Experimental Procedures

2.1 Materials

AZ91 with a composition of 9.0% Al, 0.68% Zn, 0.33% Mn, 0.1% Si, and 0.03% Cu, was used as the matrix. The Pr (~200 mesh) and AZ91 (~300 mesh) powders (Figure 1) were prepared as raw powders. In this investigation, the magnesium alloy, rare earth Pr and multi-walled CNTs were used to produce metal matrix composites using a powder metallurgy method. The addition of Pr was 1.0 wt.%. The raw materials utilized were multi-walled carbon nanotubes (20 to 200 nm in diameter and approximately 30 μm in length, purity > 95 wt.%). The functional groups of –COOH and –OH were added on the surface of raw CNTs.

2.2 Coating Process

Multiwalled CNTs were CNTs were immersed in HNO_3 (65% purity) and refluxed at 140 °C for 3 h, hereafter named as acid-treated CNTs [22–24]. After acid treatment, washing in distilled water and drying (Figure 2), the CNTs are placed in ethanol and sealed. A uniformly dispersed CNT/ethanol solution was obtained using ultrasonic mixing for 1 h (power: 90 W). Glycerol is added dropwise to the solution as it is being ultrasonically processed. Next, tetrabutyl titanate was added to the ultrasonically stirred mixture. The solution was placed in a reaction vessel and heated in a muffle furnace for 12 h at 180 °C, and cooled in air. The solution was centrifuged using anhydrous ethanol until the solution was colorless, and then centrifuged another 3 to 5 times. The obtained solid phase material was dried at 70 °C to obtain a CNT precursor coated with TiO_2. Finally, the precursor was sintered under argon atmosphere at 450 °C for 2 h to obtain TiO_2@CNT. X-ray diffraction (XRD) was used to determine the crystal structure of the coating. Scanning electron microscopy (SEM) and transmission electron microscopy (TEM) were used to study the microstructure of the CNTs after coating.

2.3 Composite Manufacturing

AZ91 alloys reinforced with 0.5, 1.0, 1.5 wt.% CNTs and 1.0 wt.% Pr [21, 25] were used. The ball-milling experiments were carried out in a planetary mechanical milling apparatus. The mixture of CNTs, AZ91, and

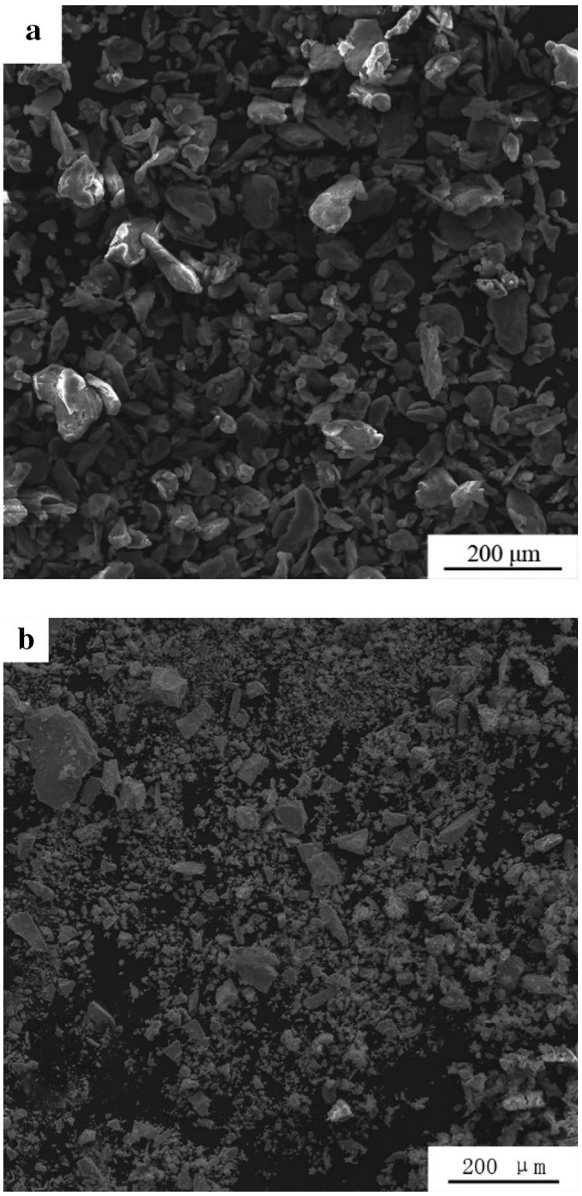

Figure 1 SEM images of raw materials: **a** AZ91 and **b** Pr

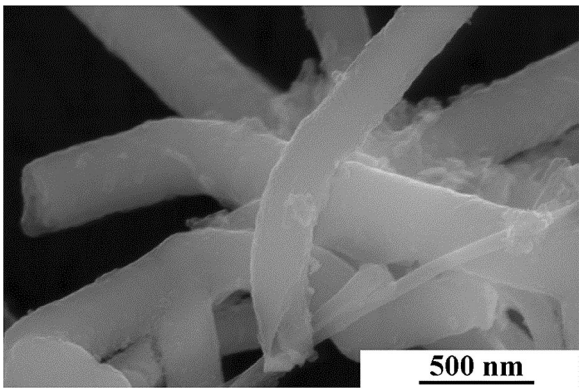

Figure 2 SEM image of CNTs after acid treatment

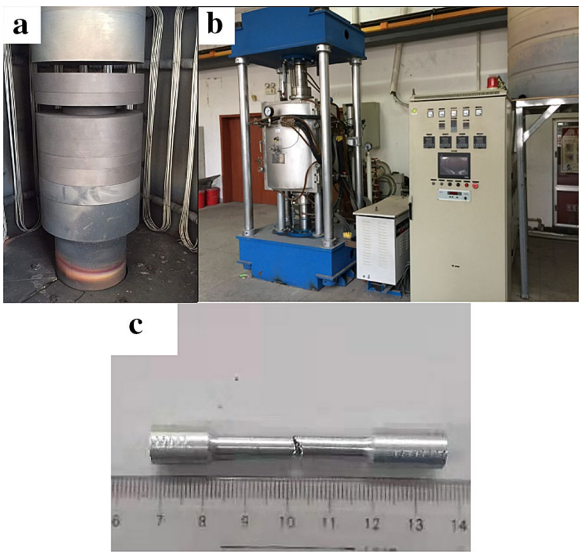

Figure 3 Tooling and machine used for the hot press process: **a** graphite die, **b** vacuum hot press, and **c** corresponding tensile specimen

Pr powders was milled at 300 rpm for 6 h in argon. The synthesized AZ91-Pr-CNT powders were hot pressed in a graphite die (as Figure 3a shown) under vacuum at a temperature of 460 °C under a pressure of 23 MPa for 1.5 h. The vacuum hot press is shown in Figure 3b. The hot-pressed composite ingots were formed cylinders with dimensions of ϕ40 mm × 20 mm. Then, the ingot was put into the extrusion die and preheated to 400 °C. The extrusion ratio was 400:16. Boron nitride was used as a lubricant. Finally, rod-shaped composites of 8 mm were obtained.

2.4 Nanocomposite Characterization

The hardness of the hot-extruded composites was measured using a HVS-1000A Vickers hardness instrument. The set load was 300 g and the duration was 10 s. A Nikon Eclipse MA200 (Nikon Metrology, Inc., Brighton, UK) optical microscope (OM), scanning electron microscopy (SEM) and transmission electron microscopy (TEM) were used to study the microstructure of the composite and the distribution of CNTs. The samples used for OM examination were mounted and then polished and etched in an ethanol solution composed of 4 vol.% nitric acid. Specimens for TEM observation were first prepared by grinding-polishing the sample to produce a foil of 50 μm thickness followed

by punching 3 mm diameter disks, and then shaved to thinner dimensions by ion beam.

2.5 Tensile Testing

To evaluate tensile properties, the test samples were machined into tensile test bars with a diameter of 5 mm and a gauge length of 25 mm, according to the ASTM E8 M05 specification. This was carried out at room temperature using a SUNC UM5105 electro-servo testing machine with a tensile speed of 0.1 mm/min. The tensile property data of yield strength (YS) ultimate tensile strength (UTS), and elongation were based on an average of 3–5 tests.

3 Results and Discussion

3.1 Coatings

It can be seen from Figure 2 that the outer surface of the CNT is relatively smooth and flat before the coating process. Via SEM, the morphology after coating of CNTs is shown in Figure 4. A large number of thorn-like projections are distributed on the outer surface of the CNT. After the coating treatment, the CNTs still maintain a complete columnar shape. It can be seen that the integrity of the CNTs remains intact. This coating process does not destroy the integrity of the CNTs. From the distribution of the thorns on the outer surface of the columnar CNTs, the distribution is shown to be relatively uniform (Figure 4a). These thorns grow uniformly on the surface of the CNTs and are connected to the CNTs via chemical bonds rather than simply stacking and adhering to the surface of the CNTs. Figure 4b shows that the surface of the CNTs remain intact and no defects, such as holes, were found.

What we desire is an arm exoskeleton which is capable of following motions of the human upper-limb accurately and supplying the human upper-limb with proper force feedback if needed. In order to achieve an ideal controlling performance, we have to examine the structure of the human upper-limb.

To determine the elemental composition of the thorns coated on the surface of the CNTs, EDS analysis was performed on the coated CNTs, as shown in Figure 4a. Figure 5 shows the results of the EDS analysis. It is shown that thorn-like protrusions on the surface of the CNTs contain three elements of C, O, and Ti.

Figure 6 presents the XRD patterns of the CNTs before and after the coating process. The TiO_2 diffraction peaks remain similar to the original CNT before coating, so the thorn coating on the surface of the CNTs is mainly TiO_2. There are sharp characteristic peaks at the 2θ angle of 26.01° and 42.91°, which can be associated with the (002) and (100) planes of carbon, respectively. Furthermore, the lower diffraction peaks at 2θ at 38°, 47.7°, 54.8°, and 62.6° of the CNTs after coating are indexed to the TiO_2 (004), (200), (211), and (204) planes, respectively.

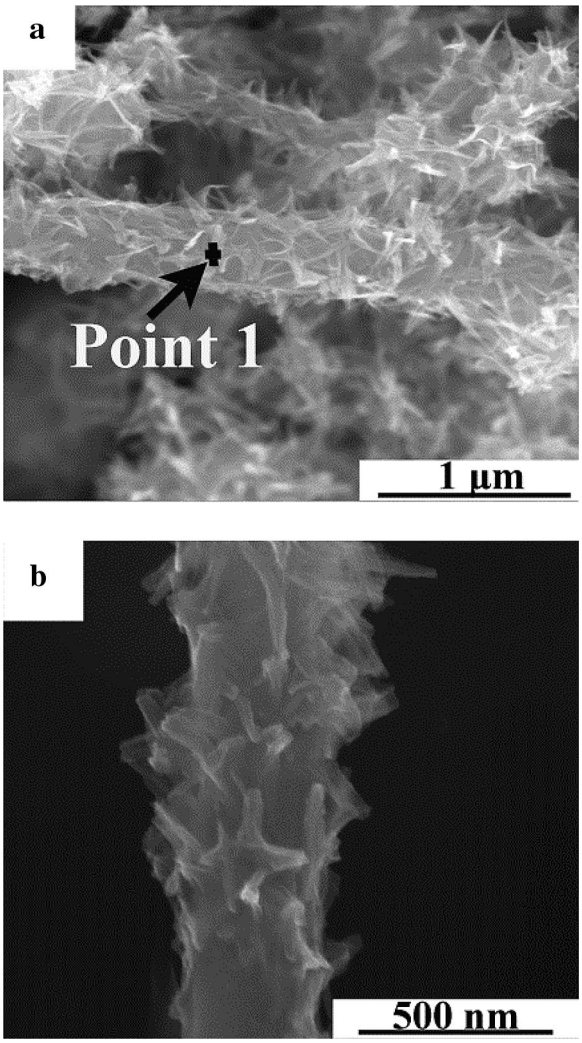

Figure 4 SEM image of CNTs after the coating process: **a** multiple CNTs, **b** single CNTs

It can be seen from Figure 7a that the diameter of the carbon nanotubes is about 200 nm, and many thorns are uniformly coated on the surface of the CNTs. Figure 7b shows the high-resolution TEM morphology of the CNTs after the coating process corresponding to the rectangular region in Figure 7a. The morphology of the CNTs lattice is clearly visible in the figure, and it is found that the outer wall of the carbon nanotube is relatively complete, indicating that the coating process does not destroy the integrity of the CNTs. From the lattice data, it can be found that TiO_2 is coated on the surface of the CNTs, and the interfacial bonding with CNTs is better. These properties of CNTs ensure good reinforcing effects in the Mg matrix composites.

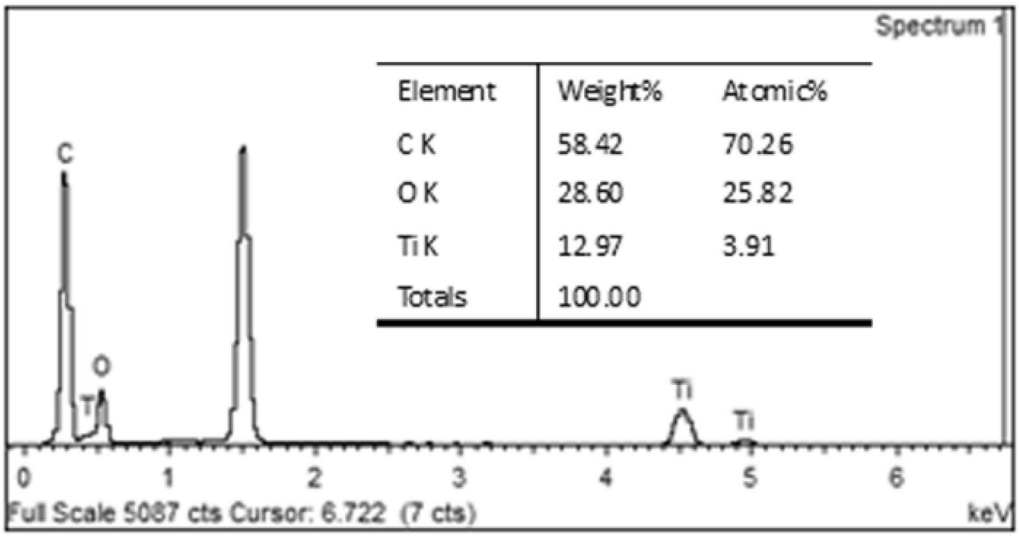

Figure 5 EDS results of point 1 in Figure 4a

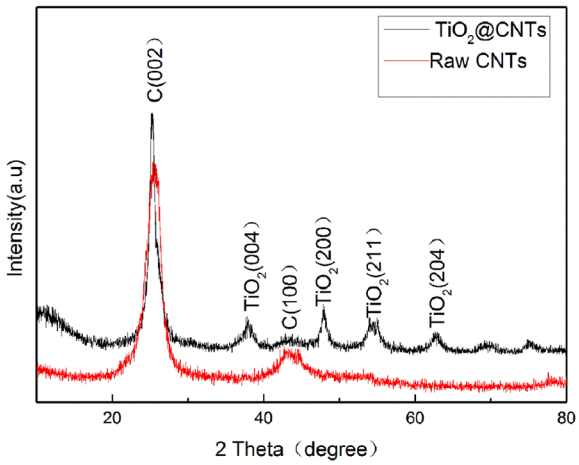

Figure 6 XRD patterns of the CNTs before and after coating process

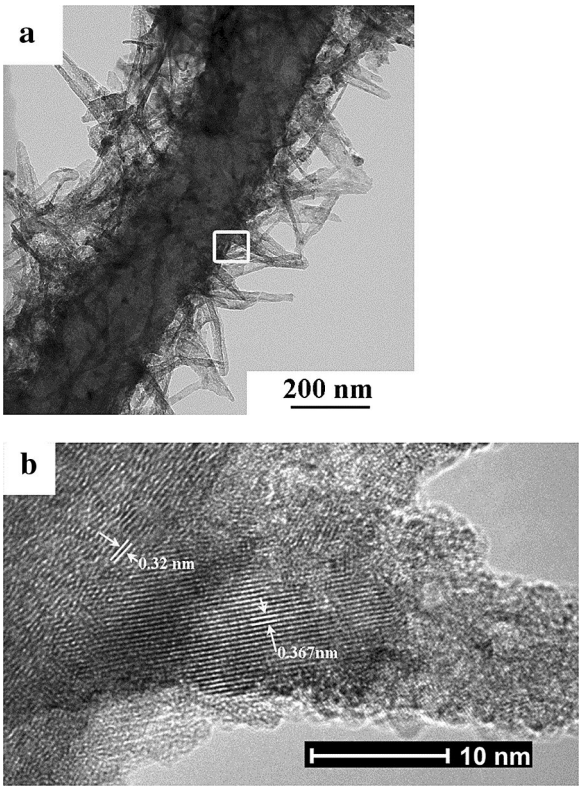

Figure 7 TEM images of the CNTs after the coating process: **a** low magnification, **b** high magnification

3.2 Composite Properties

3.2.1 Microstructure

Figure 8 is a microstructure of an AZ91 alloy reinforced by uncoated CNTs and Pr after hot pressing. The content of CNTs is 1.0 wt.%. Although the mechanical milling and hot pressing sintering are carried out, the added CNTs are not well dispersed. Significant agglomeration of CNTs can be observed in Figure 8. If the CNTs are not subjected to a surface coating treatment, the CNTs are difficult to disperse uniformly in the magnesium alloy matrix, due to poor wettability [26]. Poor wettability also leads to poor interfacial bonding strength of the uncoated CNT and magnesium matrix alloy [27].

Figure 9 shows the TEM images of the AZ91 alloy reinforced byTiO_2@CNTs and Pr. It can be found that the CNTs after coating treatment have a good bonding

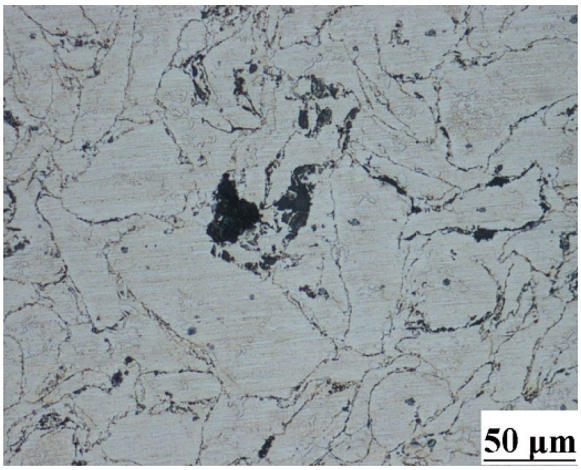

Figure 8 Microstructure of AZ91-Pr alloy reinforced by uncoated CNTs after hot press

interface with the matrix in the composite. It was clearly observed that no significant morphological damage was observed in the CNTs, and the integrity of the CNTs was maintained. There are no pores at the interface between the CNTs and the matrix. This indicates a good interfacial bond between the CNTs and matrix. Through the measurement of the lattice spacing, the interval between the stripes measured in Figure 9b is 0.235 nm, corresponding to the TiO_2 (004) plane. It was further verified that TiO_2 was successfully coated on the surface of CNTs and helped to enhance the interfacial bonding between CNTs and the magnesium alloy matrix. Figure 10 is the High-Angle Annular Dark Field (HAADF) STEM image of AZ91-Pr-1.0TiO_2@CNTs alloy. It can be seen that the C element is relatively uniformly dispersed in the alloy, and the dispersion of CNTs in the matrix is relatively uniform. It can also be observed that the rare earth element Pr is distributed on the grain boundaries.

Figure 11 shows optical microstructures of tested composites after vacuum hot pressing sintering and extrusion. It can be seen from Figure 11a that the composite after hot pressing sintering, the added TiO_2@CNTs are mainly distributed at the α-Mg grain boundaries. The island or block shape β-$Al_{17}Mg_{12}$ phase is distributed at the α-Mg grain boundary. The addition of Al in the rare earth Pr and AZ91 magnesium alloy forms the $Al_{11}Pr_3$ phase, and its morphology is long needle-like. By addition of the Pr elements, a lower amount of aluminum could become available for the formation of β phase, subsequently, leading to a change in the morphology of this phase [21]. After extrusion, a black strip region appears on the surface of the alloys. The black strip is mainly caused by the orientation of the TiO_2@CNTs along the extrusion direction. CNTs may lead to a significant

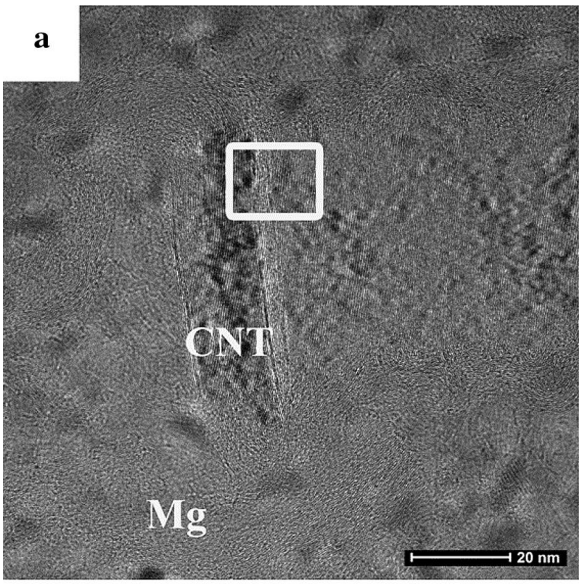

Figure 9 TEM images of the AZ91-Pr-TiO_2@CNTs composite: **a** low magnification, **b** high magnification

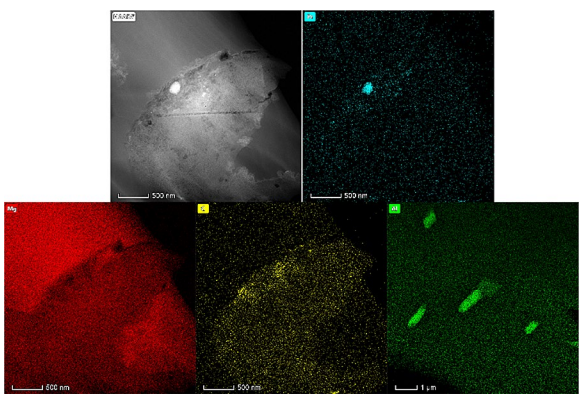

Figure 10 The High-Angle Annular Dark Field (HAADF) STEM image of AZ91-Pr-1.0 TiO_2@CNTs composite

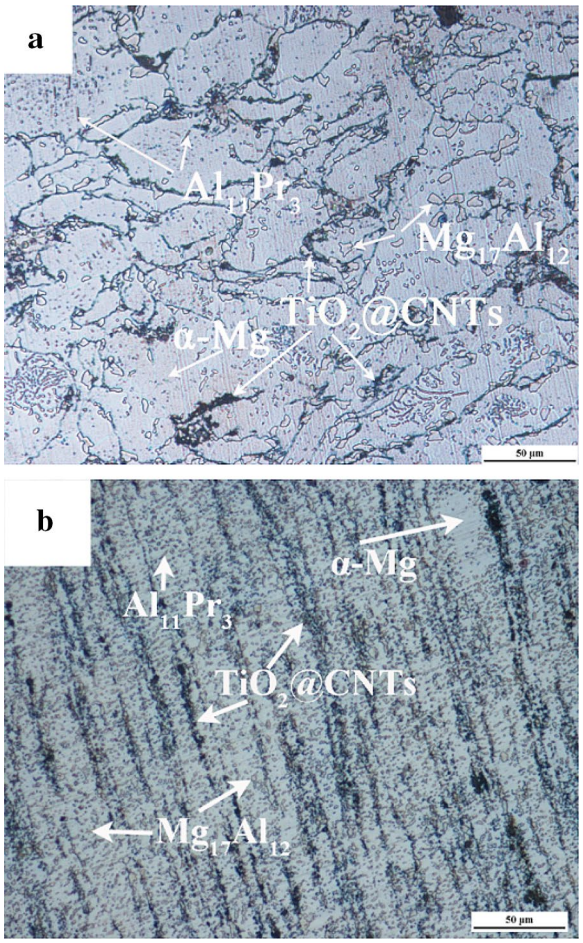

Figure 11 Optical micrographs of AZ91-Pr-1.0 TiO_2@CNTs composites after vacuum hot pressing sintering (**a**) and extrusion (**b**)

inhibition in grain boundary migration of the composite resulting in refined grains after extrusion [28]. Large amounts of bulk β-$Mg_{17}Al_{12}$ particles were broken during the hot extrusion process, with most of them finally distributing along the recrystallized grain boundaries [29]. The β-$Mg_{17}Al_{12}$ promotes DRX nucleation and inhibits grain growth during hot extrusion, which results in fine grain size [30]. The distribution of TiO_2@CNTs in the composite tends to be uniform after hot extrusion.

3.2.2 Mechanical Properties

Tensile properties at room temperature of the AZ91 with TiO_2@CNTs and Pr additions are shown in Table 1. Since the reinforcing particles have a pinning effect on the dislocation during the deformation process, the addition of rare earth Pr can increase the UTS and YS of the AZ91 matrix, but the elongation is slightly decreased. Moderate improvement in UTS (32.8%), YS (4.9%), and elongation (12.8%) are observed with 0.5 wt.% CNT added to

Table 1 Tensile properties of the experimental alloys at room temperature

Alloy	YS (MPa)	UTS (MPa)	%E
AZ91	157.23	213.96	5.0
AZ91-Pr	172.39	261.32	4.7
AZ91-Pr-1.0 CNTs	174.63	258.47	4.5
AZ91-Pr-0.5CNTs@TiO_2	180.77	346.99	5.3
AZ91-Pr-1.0CNTs@TiO_2	194.19	389.67	7
AZ91-Pr-1.5CNTs@TiO_2	190.12	377.76	6.7

the AZ91-Pr alloy. When the addition of TiO_2@CNTs was 1 wt.%, UTS, YS, and elongation reached maximum values of 194.19 MPa, 389.67 MPa, and 7%, respectively. The strengthening effect of CNTs helps the alloy resist tensile stress, while the addition of TiO_2@CNTs refines the grains and improves the plasticity of the alloy, hence improving the elongation of the alloy. When the addition of TiO_2@CNTs is 1.5 wt.%, the distribution of TiO_2@CNTs is uneven due to agglomeration and the grain size increases. Therefore, the mechanical properties and elongation of the alloy are reduced.

The distribution of TiO_2@CNTs in the matrix alloy is mainly divided into three morphologies, as shown in Figure 12a, b, c: single, multiple, and large number of agglomerates. In the single or multiple cases, TiO_2@CNTs are arranged along the extrusion direction during the extrusion process. TiO_2 is uniformly distributed on the surface of CNTs and is dense. The TiO_2 on the surface

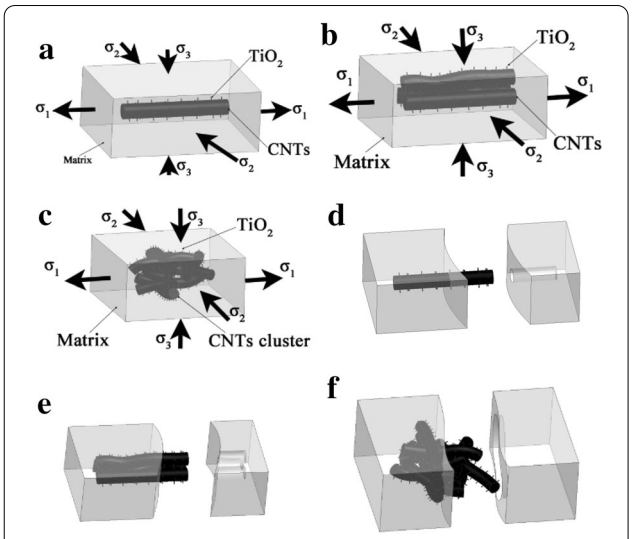

Figure 12 Schematics of the TiO2@CNTs distribution in AZ91-Pr alloy during the tensile test: **a** single CNTs, **b** multiple CNTs, **c** CNTs cluster, **d** crack of single CNTs, **e** crack of multiple CNTs, and **f** crack of CNTs cluster

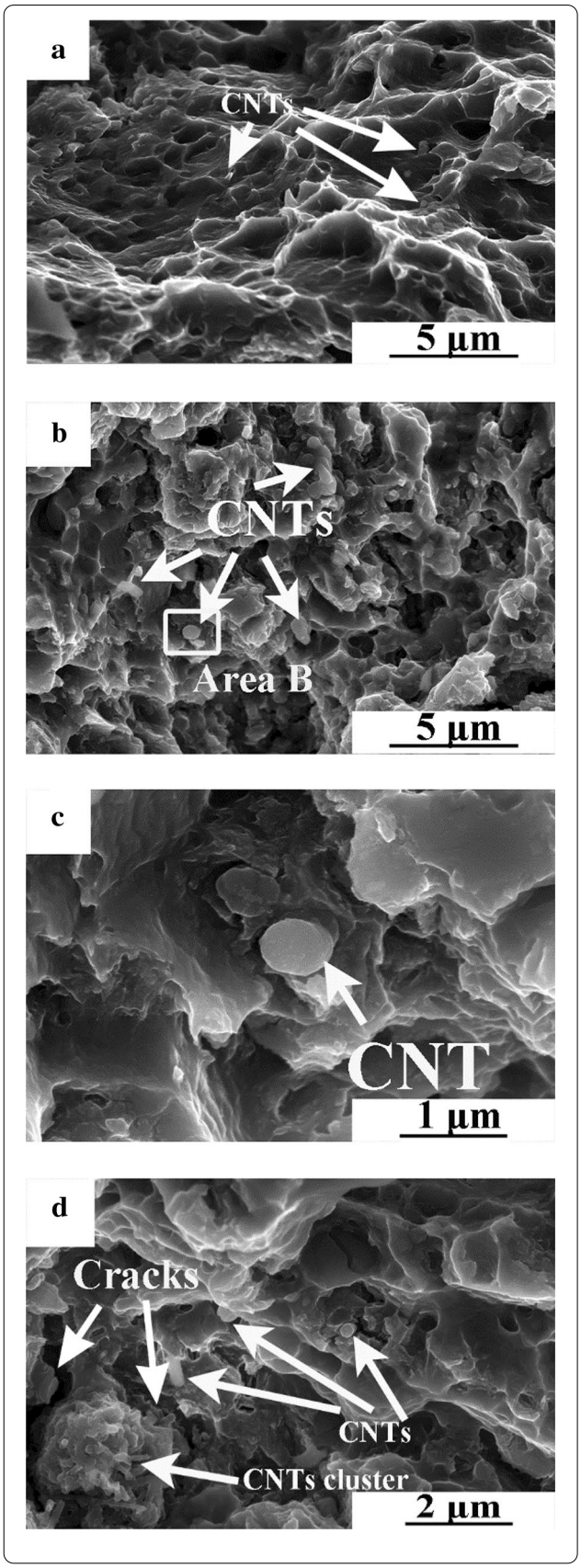

Figure 13 SEM micrographs of tensile fracture of the tested alloys: **a** AZ91-Pr-0.5 TiO_2@CNTs, **b** AZ91-Pr-1.0 TiO_2@CNTs, **c** the magnified images of area B in (**b**), and **d** AZ91-Pr-1.5 TiO_2@CNTs

of the CNTs acts as a pinning mechanism to firmly affix the CNTs in the matrix. During the stretching process, the tensile stress applied to the magnesium matrix alloy passes through the TiO_2 protrusions on the surface of the CNTs, transferring the force to the CNTs. Therefore, the advantages of the CNTs can be realized, and the ultimate tensile stress of the alloy is remarkably improved. As Figure 12d, e shown, when the stress exceeds the interfacial bonding strength between TiO_2 and the matrix alloy, the alloy breaks. However, when CNTs are agglomerated, TiO_2@CNTs are not arranged in the extrusion direction due to the intertwining of the agglomerated CNTs. The agglomerated CNTs do not enhance the properties of the alloy but become a derivative of the crack during the stretching process, as shown in Figure 12f. When there are a large number of agglomerated CNTs in the alloy, the ultimate tensile strength of the alloy decreases. The addition of TiO_2@CNTs has a limited increase in the yield strength of the alloy, and the yield strength of the alloy is mainly determined by the matrix alloy.

For the same CNTs content, whether or not to carry out coating pretreatment has a significant effect on the mechanical properties of the composite. When the uncoated CNTs are added to AZ91-Pr, the yield strength will increase slightly, but the ultimate tensile strength will decrease. The uncoated CNTs have a certain reinforcing effect on the composite material before plastic deformation. However, when cracks occur inside the material due to tensile stress, the agglomerated CNTs cannot pin the crack and may even accelerate the crack propagation. Therefore, the ultimate tensile strength of the composite material is lowered and the elongation is also slightly decreased. The addition of coated TiO_2@CNTs can improve the mechanical properties of the material. It can be seen that TiO_2 coated on CNTs plays a good role in transferring the tensile force and plays a key role in enhancing the mechanical properties of the material.

3.2.3 Fracture

The alloy tensile fractures are shown in Figure 13. Figure 13a shows the fracture morphology of AZ91-Pr-0.5 TiO_2@CNTs alloy, and the presence of carbon nanotubes can be seen from the fracture morphology. Since TiO_2@CNTs can increase the tensile strength of the alloy, the fracture surface usually appears at a position where the TiO_2@CNTs is less in the cross section. Therefore, fewer CNTs are seen on the fracture surface. The orientation of the added carbon nanotubes

are formed in the extrusion direction during the extrusion process. This helps to resist the stresses experienced by the tensile process and can increase the UTS of the alloy. Figure 13b shows the SEM micrographs of tensile fracture of the AZ91-Pr-1.0 TiO_2@CNTs alloy, where more carbon nanotube distribution can be seen from the fracture, and the UTS of the alloy continues to increase. However, the fracture surface of the specimens shows a tendency of increasing cracks with the increase of the CNTs content. When the amount of TiO_2@CNTs added reaches 1.5 wt.%, the fracture of the alloy is as shown in Figure. 13e, and the agglomerated carbon nanotubes can be seen from the fracture. Although the number of carbon nanotubes increased, due to the agglomeration, cracks are easily generated at the agglomeration during tensile testing, resulting in a decrease in the UTS of the alloy.

4 Conclusions

In this paper, CNTs were first coated to prepare TiO_2@CNTs. Then TiO_2@CNTs and Pr reinforced AZ91 alloys were fabricated by mechanical milling, vacuum hot pressing, and hot extrusion forming processes. The effects of TiO_2@CNTs and Pr on the microstructure and mechanical properties of AZ91 alloy were investigated. The conclusions of this investigation were as follows:

1) The surface of the CNTs were coated successfully with TiO_2 by the coating process. The coated TiO_2 is evenly distributed on the surface of CNTs and adhered well with the CNTs.
2) The coated TiO_2 improved the interfacial bonding strength between the CNTs and the magnesium alloy matrix.
3) During the extrusion process, the added TiO_2@CNTs distributed along the extrusion direction form a directional orientation. TiO_2@CNTs can refine the grain of the base alloy. When the concentration of TiO_2@CNTs is 1.0 wt.%, the distribution was uniform and the grains were the finest.
4) The addition of rare earth Pr can increase the UTS and YS of the AZ91 matrix, but the elongation is slightly decreased. The addition of TiO_2@CNTs increased the UTS, YS, and elongation of the alloy. When the addition amount was 1.0 wt.%, the maximum values of 194.19 MPa, 389.67 MPa and 7%, respectively, were attained. Compared with the matrix, this showed increases of 23.5%, 82.1%, and 40.0%, respectively.
5) The fracture modes of the alloys were all cleavage fractures. The carbon nanotubes carried tensile stress, but when the TiO_2@CNTs concentration was too high, the CNT agglomerates easily formed cracks.

Acknowledgements
Not applicable.

Authors' Contributions
NL and HY conceived and designed the experiments; NL and QW performed the coating experiments; NL, HY and QW analyzed the data; NL, and ZC contributed reagents/materials/analysis tools; NL, HY, QW and ZC wrote the paper. All authors read and approved the final manuscript.

Authors' Information
Ning Li, born in 1980, is currently a lecturer at *Nanchang Hangkong University*. His main research is the modification of Al-Mg alloys. E-mail: lining@nchu.edu.cn.

Hong Yan, born in 1962, is currently a professor at *School of Mechanical-Electronic Engineering, Nanchang University, China*. He received his PhD degree from *Nanchang University, China*, in 2001. His main research is integrated technology of advanced material preparation and forming. Tel: +86 13667090600; E-mail: hyan@ncu.edu.cn.

Qingjie Wu, born in 1985, is currently a PhD at *Nanchang Hangkong University*. His main research is the modification of Al-Mg alloys. E-mail: wu856200@163.com.

Zeyu Cao, born in 1995, is currently a master candidate at *Nanchang University, China*. His main research is the modification of Al-Mg alloys. E-mail: czy1064863670@163.com.

Funding
Supported by National Natural Science Foundation of China (Grant No. 51965040), Loading Program of Science and Technology of College of Jiangxi Province (Grant No. KJLD14003).

Competing Interests
The authors declare no competing financial interests.

Author Details
[1] School of Mechanical Electrical Engineering, Nanchang University, Nanchang 330031, China. [2] School of Aviation Manufacturing Engineering, Nanchang Hangkong University, Nanchang 330069, China.

Received: 6 January 2020 Revised: 21 January 2021 Accepted: 28 January 2021
Published online: 24 February 2021

References

[1] Changlin Yang, Bin Zhang, Dongchen Zhao, et al. Microstructure evolution of as-cast AlN/AZ91 composites and room temperature compressive properties. *Journal of Alloys and Compounds*, 2019, 774: 573-580.
[2] K Evgeniya, B Salar, K Johannes, et al. Development of Al–Mg–Sc thin foils for fiber-reinforced metal laminates. *Advanced Engineering Materials*, 2019, 21(4): 1800462.
[3] Zhi Hu, R L Liu, Kairy Shravan, et al. Effect of the Sm additions on the microstructure and corrosion behavior of magnesium alloy AZ91. *Corrosion Science*, 2019, 149: 144-152.
[4] Hong Yan, Zhiwei Wang. Effect of heat treatment on wear properties of extruded AZ91 alloy treated with yttrium. *Journal of Rare Earths*, 2016, 34(3): 308-314.
[5] Y H Zhang, Z H Hou, Y Cai, et al. Structures and hydrogen storage properties of RE–Mg–Ni–Mn-based AB2-type alloys prepared by casting and melt spinning. *Rare Metals*, 2016(10): 1-11.
[6] H Yu, S N Chen, W Yang, et al. Effects of rare element and pressure on the microstructure and mechanical property of AZ91D alloy. *Journal of Alloys and Compounds*, 2014, 589: 479-484.

[7] S Nazarov, S Rossi, P Bison, et al. Influence of rare earths addition on the properties of Al–Li alloys. *The Physics of Metals and Metallography*, 2019, 120(4): 402-409.

[8] Qingjie Wu, Hong Yan. Fabrication of carbon nanofibers/A356 nanocomposites by high-intensity ultrasonic processing. *Metallurgical and Materials Transactions A*, 2018, 49(6): 2363-2372.

[9] Masuda, Chitoshi, Ogawa, et al. Microstructure evolution during fabrication and microstructure-property relationships in vapour-grown carbon nanofibre-reinforced aluminium matrix composites fabricated via powder metallurgy. *Composites, Part A. Applied Science and Manufacturing*, 2015, 71A: 84-94.

[10] M Liu, B J Rohde, R Krishnamoorti, et al. Bond behavior of epoxy resin–polydicyclopentadiene phase separated interpenetrating networks for adhering carbon fiber reinforced polymer to steel. *Polymer Engineering & Science*, 2020, 60(1): 104-112.

[11] Yeyang Xiang, Xiaojun Wang, Xiaoshi Hu, et al. Achieving ultra-high strengthening and toughening efficiency in carbon nanotubes/magnesium composites via constructing micro-nano layered structure. *Composites Part A*, 2019, 119: 225-234.

[12] Seii Oh, Junyoung Lim, Yuchan Kim, et al. Fabrication of carbon nanofiber reinforced aluminum alloy nanocomposites by a liquid process. *Journal of Alloys and Compounds*, 2012, 542: 111-117.

[13] Fukuda Hiroyuki, Kondoh Katsuyoshi, Umeda Junko, et al. Fabrication of magnesium based composites reinforced with carbon nanotubes having superior mechanical properties. *Materials Chemistry and Physics*, 2011, 127(3): 451-458.

[14] Fukuda Hiroyuki, Kondon Katsuyoshi, Umeda Junko, et al. Interfacial analysis between Mg matrix and carbon nanotubes in Mg–6 wt.% Al alloy matrix composites reinforced with carbon nanotubes. *Composites Science & Technology*, 2011, 71(5): 705-709.

[15] Shiying Liu, Feipeng Gao, Qiongyuan Zhang, et al. Fabrication of carbon nanotubes reinforced AZ91D composites by ultrasonic processing. *Transactions of Nonferrous Metals Society of China*, 2010, 20(7): 1222-1227.

[16] C D Li, X J Wang, W Q Liu, et al. Effect of solidification on microstructures and mechanical properties of carbon nanotubes reinforced magnesium matrix composite. *Materials and Design*, 2014, 58(6): 204-208.

[17] Li Zhang, Qudong Wang, Wenjun Liao, et al. Microstructure and mechanical properties of the carbon nanotubes reinforced AZ91D magnesium matrix composites processed by cyclic extrusion and compression. *Materials Science and Engineering: A*, 2017, 689: 427-434.

[18] Paramsothy Muralidharan, Xinghe Tan, Chan Jimmy, et al. Si_3N_4 nanoparticle addition to concentrated magnesium alloy AZ81: Enhanced tensile ductility and compressive strength. *Isrn Nanomaterials Isrn Nanomaterials*, 2012, 1: 111-118.

[19] H Mindivan, A Efe, AH Kosatepe, et al. Fabrication and characterization of carbon nanotube reinforced magnesium matrix composites. *Applied Surface Science*, 2014, 318: 234-243.

[20] CS Goh, J Wei, L C Lee, et al. Simultaneous enhancement in strength and ductility by reinforcing magnesium with carbon nanotubes. *Materials Science & Engineering A*, 2006, 423(1-2): 153-156.

[21] N Li, H Yan. The effects of rare earth Pr and heat treatment on the wear properties of AZ91 alloy. *Crystals*, 2018, 8(6): 256-268.

[22] Q H Yuan, X S Zeng, Y Liu, et al. Microstructure and mechanical properties of Mg-4.0Zn alloy reinforced by NiO-coated CNTs. *Materials Science and Technology*, 2017, 33(5): 452-460.

[23] Alicia Moya, Alexey Cherevan, Silvia Marchesan, et al. Oxygen vacancies and interfaces enhancing photocatalytic hydrogen production in mesoporous CNT/TiO_2 hybrids. *Applied Catalysis B: Environmental*, 2015, 179: 574-582.

[24] F P Du, H Tang, D Y Huang. Thermal conductivity of epoxy resin reinforced with magnesium oxide coated multiwalled carbon nanotubes. *International Journal of Polymer Science*, 2013(15): 9714-9722.

[25] Jianing Liu, Dong Bian, Yufeng Zheng, et al. Comparative in vitro study on binary Mg-RE (Sc, Y, La, Ce, Pr, Nd, Sm, Eu, Gd, Tb, Dy, Ho, Er, Tm, Yb and Lu) alloy systems. *Acta Biomaterialia*, 2020, 102: 508-528.

[26] Kondon Katsuyoshi, Fukuda Hiroyuki, Umeda Jumko, et al. Microstructural and mechanical analysis of carbon nanotube reinforced magnesium alloy powder composites. *Materials Science & Engineering: A*, 2010, 527(16-17): 4103-4108.

[27] Qiuhong Yuan, Xiaoshu Zeng, Yong Liu, et al. Microstructure and mechanical properties of AZ91 alloy reinforced by carbon nanotubes coated with MgO. *Carbon*, 2016, 96(1): 843-855.

[28] CD Li, XJ Wang, WQ Liu, et al. Microstructure and strengthening mechanism of carbon nanotubes reinforced magnesium matrix composite. *Materials Science and Engineering A*, 2014, 597(1): 264-269.

[29] Zhifeng Li, Jie Dong, Xiaoqing Zeng, et al. Influence of $Mg_{17}Al_{12}$ intermetallic compounds on the hot extruded microstructures and mechanical properties of Mg–9Al–1Zn alloy. *Materials Science and Engineering A*, 2007, 466(1-2): 134-139.

[30] Cuiju Wang, Kunkun Deng, Kaibo Nie, et al. Competition behavior of the strengthening effects in as-extruded AZ91 matrix: Influence of pre-existed $Mg_{17}Al_{12}$ phase. *Materials Science and Engineering A*, 2016, 656: 102-110.